

## Dual energy converting nano-phosphors: upconversion luminescence and X-ray excited scintillation from a single composition of lanthanide-doped yttrium oxide

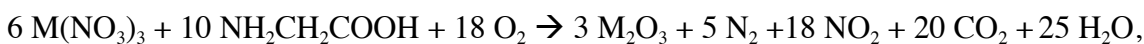
Ian N. Stanton, Jennifer A. Ayres, Michael J. Therien\*

Department of Chemistry, French Family Science Center, 124 Science Drive,  
Duke University, Durham, North Carolina, 27708 USA

### Experimental:

**Materials.**  $\text{Y}(\text{NO}_3)_3 \cdot 6\text{H}_2\text{O}$  (99.8%),  $\text{Yb}(\text{NO}_3)_3 \cdot 5\text{H}_2\text{O}$  (99.9%),  $\text{Er}(\text{NO}_3)_3 \cdot 5\text{H}_2\text{O}$  (99.9%),  $\text{Li}(\text{NO}_3)$  (99.99%), and glycine ( $\geq 99\%$ ) were purchased from Sigma-Aldrich and used without further purification. HPLC-grade  $\text{H}_2\text{O}$  was also used (Fisher Chemicals).

**Synthesis of  $[\text{Y}_2\text{O}_3; \text{Ln}]$ .**  $[\text{Y}_2\text{O}_3; \text{Yb} (2\%), \text{Er} (1\%)]$  and  $[\text{Y}_2\text{O}_3; \text{Yb} (2\%), \text{Er} (1\%), \text{Li} (5\%)]$  were synthesized by a solution combustion synthesis involving glycine as the fuel. The reaction is as follows;



where  $\text{M} = \text{Y}, \text{Yb}, \text{Er}, \text{or Li}$ . The glycine-to-metal nitrate molar ratio was kept at 1.5:1 to ensure consistency of the samples. In a typical synthesis, 25 ml of HPLC grade  $\text{H}_2\text{O}$  was used to dissolve a total 0.2 mol/L of metal-nitrates and 0.3 mol/L of glycine in a 100 ml beaker. **Table 1** shows the amounts based on this method for  $[\text{Y}_2\text{O}_3; \text{Yb} (2\%), \text{Er} (1\%)]$ .

**Table 1.** Theoretical amounts of precursors for  $[\text{Y}_2\text{O}_3; \text{Yb} (2\%), \text{Er} (1\%)]$  based on a 25 ml solution.

	$\text{Y}(\text{NO}_3)_3 \cdot 6\text{H}_2\text{O}$	$\text{Yb}(\text{NO}_3)_3 \cdot 5\text{H}_2\text{O}$	$\text{Er}(\text{NO}_3)_3 \cdot 5\text{H}_2\text{O}$	glycine
mol / L (25 ml $\text{H}_2\text{O}$ )	0.194	0.004	0.002	0.3
Mass (g)	1.858	0.045	0.022	0.563

After stirring until completely dissolved, the stir bar was removed and the reaction was placed on a hot plate set to maximum heat until combustion occurred, which took approximately 15 minutes. For safety purposes, the beaker and hot plate were enclosed by ½ inch plexi-glass box during the reaction. Once the reaction occurred, the beaker was immediately removed from the hot plate and allowed to cool to room temperature. While most of the nanoparticle product remained in the beaker, a small amount of the white powder was also dispersed within the plexi-glass enclosure. All powders were then

collected in an aluminum oxide crucible and placed in a furnace at 500 °C for 1 hour under normal atmospheric conditions to burn off any residual nitrates. The powders were then experimentally tested as is.

### **Instrumentation:**

X-ray Diffraction (XRD), Scanning Electron Microscopy (SEM), and Transmission Electron Microscopy (TEM) were performed at the *Shared Materials Instrumentation Facility* (SMiF) at Duke University.

**X-ray Diffraction.** Powder XRD was measured on a Philips X'Pert PRO MRD HR X-Ray Diffraction System from 25° - 75° (2 $\theta$ ) under Cu K-Alpha (1.542 Å) irradiation at 45 keV and 40 mA.

**Scanning Electron Microscopy.** SEM was performed on a FEI XL30 SEM-FEG with a field emission source operating at 30 keV.

**Transmission Electron Microscopy.** TEM images were acquired on a FEI Tecnai G<sup>2</sup> Twin microscope operated at an accelerating voltage of 200 keV and equipped with a TIA digital camera. Sample preparation consisted of making a 1 mg/mL solution of bare nanocrystals in ethanol, sonicating the solution for 1 minute in a bath sonicator, and then placing several drops of this solution on a carbon-formvar 400 mesh copper grid (EMS).

**Upconversion Luminescence (UCL).** UCL spectra were measured on an Edinburgh FLSP920 equipped with a Hamamatsu R2658 PMT. Solid samples (5 mg) were mounted in the spectrometer using a 100 micrometer Starna Cell powder sample holder and excited using an OEM Laser Systems 980 nm laser diode with tunable power. The emissions from the powder were passed through a Schott KG-5 filter to minimize scatter noise from high excitation densities and spectra were collected from 350-680 nm. All spectra were corrected for spectral throughput and detector sensitivity based on calibrations from a NIST calibrated light source provided by Edinburgh Instruments.

**X-ray Excited Scintillation (XES).** XES spectra were measured on an Edinburgh FLSP920 equipped with a Hamamatsu R2658 PMT over the range from 350 – 680 nm. A Faxitron RX-650 X-Ray Cabinet fiber coupled (Ocean Optics 400  $\mu$ m) to the Edinburgh FLSP920 detection system allows for XES measurements with excitation powers ranging from 30 - 130 keV at a constant current of 5 mA. For measurements, 5

*Supporting Information*

Stanton, Ayres, & Therien

mg of powder were pressed into a 7 mm diameter pellet using a Pike Technologies' hand press and placed on a piece of Teflon in the x-ray cabinet. The sample was aligned with the mounted fiber for maximum light collection; optimum alignment was verified by maximizing the emission intensity for each sample.

**Figure S1.** X-ray diffraction patterns of **Yb<sub>2</sub>Er<sub>1</sub>** (A), **Yb<sub>2</sub>Er<sub>1</sub>Li<sub>5</sub>** (B) and **Yb<sub>10</sub>Er<sub>1</sub>** (C). These spectra match the JCPDS-88-1040 Index for cubic yttrium oxide demonstrating all compositions are crystalline and cubic.

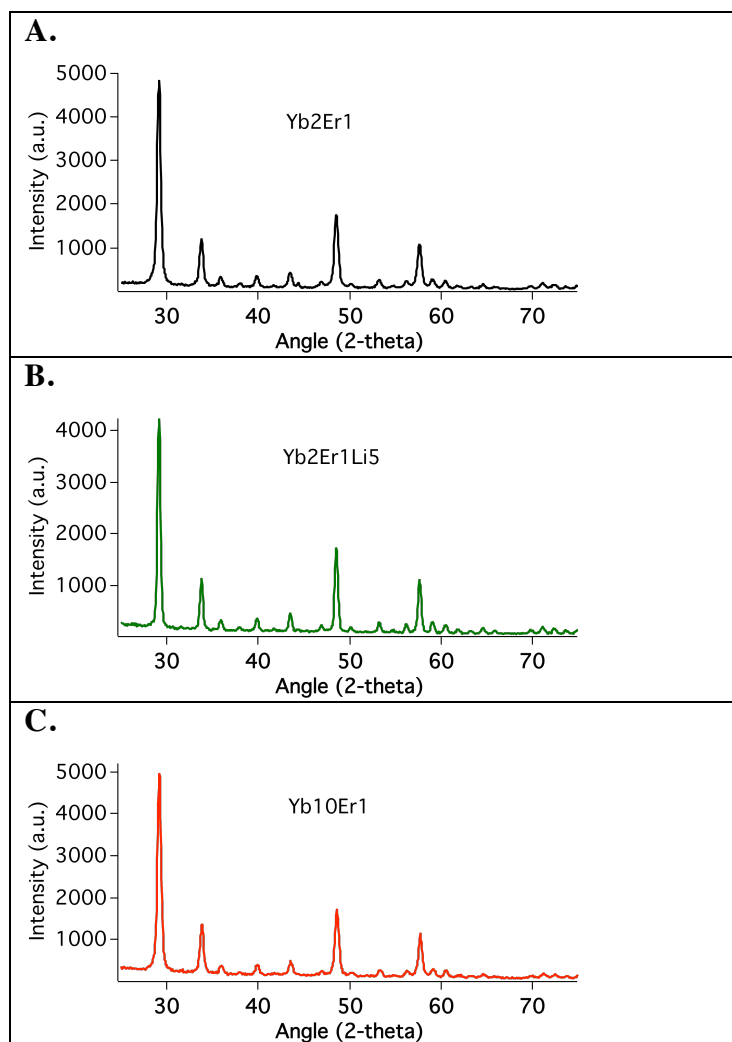


**Figure S2.** Exemplar SEM images of **Yb<sub>2</sub>Er<sub>1</sub>** (A), **Yb<sub>2</sub>Er<sub>1</sub>Li<sub>5</sub>** (B), and **Yb<sub>10</sub>Er<sub>1</sub>** (C), highlighting the small, individualized nanocrystals as well as the micron sized “coral-like” structures present in both samples with and without lithium.

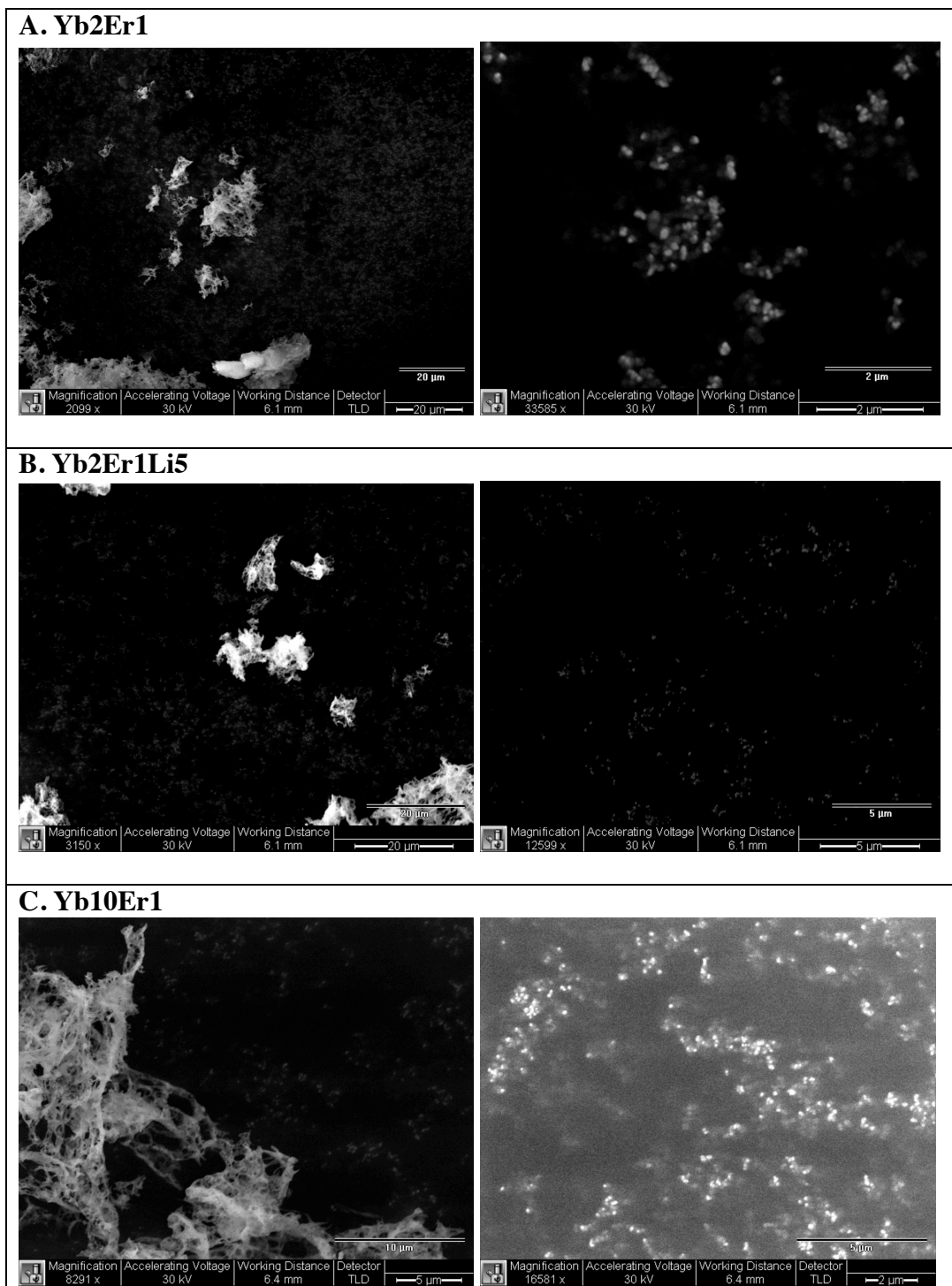


**Figure S3.** Additional TEM images of **Yb<sub>2</sub>Er<sub>1</sub>** (A) and **Yb<sub>2</sub>Er<sub>1</sub>Li<sub>5</sub>** (B), showing how the micron-sized structures are actually composed of nanocrystallites. This further shows the effects of Li-doping, as the **Yb<sub>2</sub>Er<sub>1</sub>Li<sub>5</sub>** nanocrystals feature larger size and better particle crystallinity than their **Yb<sub>2</sub>Er<sub>1</sub>** parent structures.

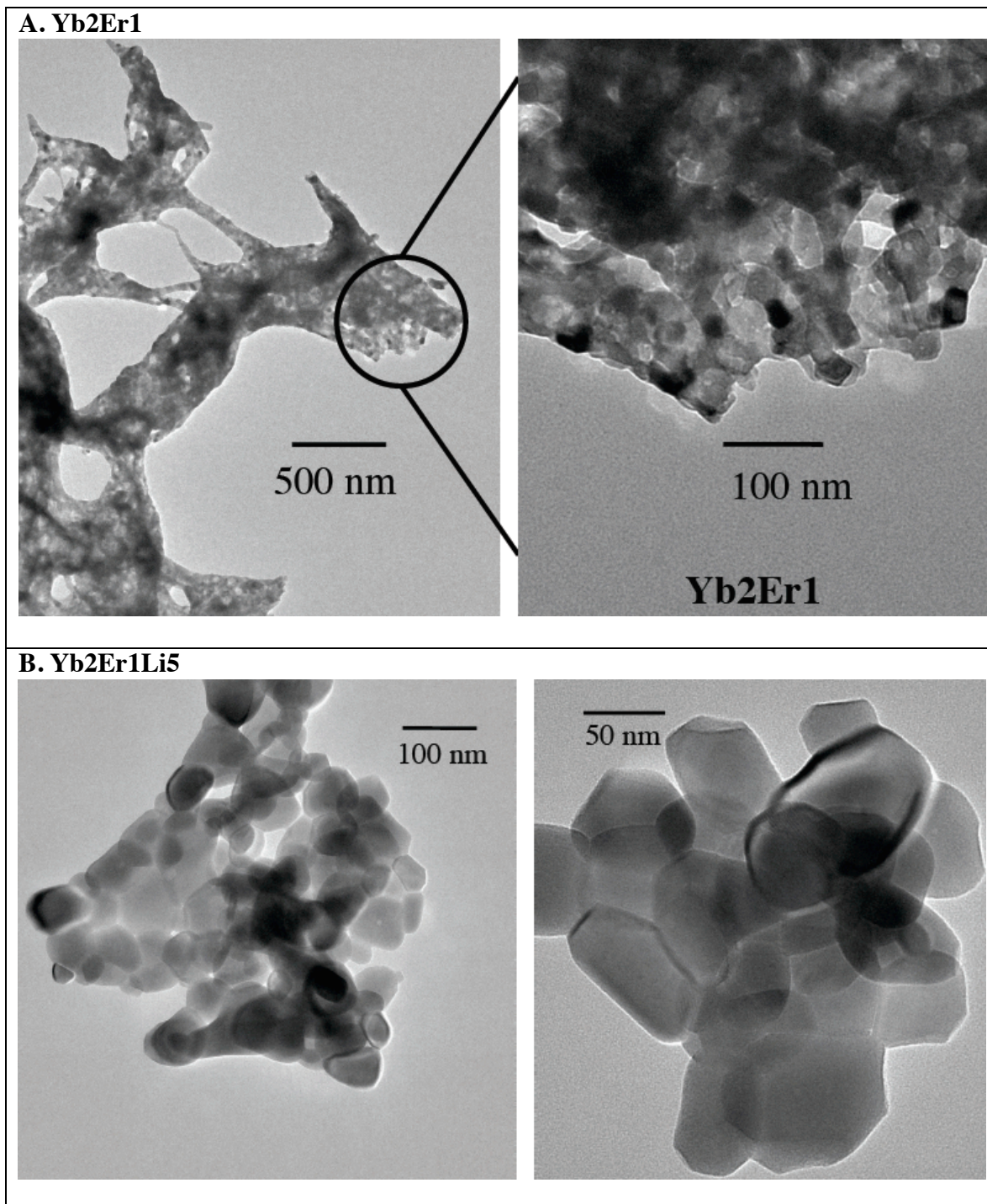


**Figure S4.** Power-dependent integrated upconversion luminescence intensity of **Yb2Er1** (A), **Yb2Er1Li5** (B), and **Yb10Er1** (C) over the green [ $^2H_{11/2}/\rightarrow ^4I_{15/2}; ^4S_{3/2}/\rightarrow ^4I_{15/2}$ ; 515 – 570 nm] and red [ $^4F_{9/2} \rightarrow ^4I_{15/2}$ ; 645 – 690 nm] centered emission lines.

